Performance Analysis of Convolutionally Coded DS-CDMA Systems with Spatial and Temporal Channel Correlations

Jie Lai and Narayan B. Mandayam
Wireless Information Network Laboratory (WINLAB)
Department of Electrical & Computer Engineering
Rutgers University
73 Brett Road, Piscataway, NJ 08854-8060

Abstract

Combined spatial and temporal processing has been shown to increase the potential link capacity enormously for wireless communication systems, especially when the channels between different transmit and receive antenna pairs are uncorrelated. In this paper, we consider both spatial and temporal channel correlations that may be encountered in space-time processing and present the performance analysis of convolutionally coded DS-CDMA systems. An upper bound for the average bit error probability ($\overline{P}_b$) is derived for the case of perfect channel estimation and an analytical approximation for $\overline{P}_b$ is derived in the case of erroneous channel estimates. The analytical approach is general enough to be applicable to various space and time diversity situations, such as wideband multipath channels and antenna arrays.

Keywords: Space-time processing, Convolutional codes, Correlated channels, CDMA

This work was supported in part by the NSF under grant number NCR 97-06036.

1 Introduction

Space-time processing has been shown to yield tremendous capacity gains in multiple-input and multiple-output (MIMO) wireless communication systems, especially when the transfer functions between different transmit and receive antenna pairs are uncorrelated [1–3]. The coherent rake receiver with pilot-aided channel estimation will be used to improve the reverse link performance versus the non-coherent rake receiver in wideband DS-CDMA based third-generation cellular systems. Most of the analytical studies in the literature on the performance of convolutional codes in DS-CDMA systems do not consider channel correlation and channel estimation errors. The usual assumptions are spatially uncorrelated multipaths/antenna signals, temporally independent symbol errors by perfect interleaving and perfect channel estimation. In the absence of the above idealistic assumptions, performance of such systems will be degraded. In practice, the temporal correlation in each fading path could be caused by imperfect interleaving due to application delay constraints. The spatial correlation between different rake fingers could exist when multipath components and their associated fingers are close to each other or the fingers come from different antennas with limited spacing in the case of antenna diversity. It has been shown in [4, 5] that spatial correlation between signals at different antenna elements may limit potential capacity gains. Thus it is of interest to analyze the performance of convolutional codes in DS-CDMA systems with spatial and temporal channel correlations. Further, since the success of space-time processing relies on accurate channel estimates, it is also of interest to study the performance under channel estimation errors.

In previous work, the performance analysis of CDMA systems has been conducted extensively [6–8]. The union bound has been used to analyze the coding performance in DS-CDMA systems under perfect channel state information and memoryless fading [7, 8]. The coding performance over non-independent Rician fading channels has been studied with perfect channel information [9]. Pairwise error probability of non-interleaved codes over Rayleigh channel with channel estimation was analyzed in [10] for a general maximum likelihood (ML) decoder. In this paper, considering the effect of temporal and spatial channel correlations, we

first derive an upper bound for the average bit error probability for a convolutionally coded DS-CDMA system under perfect channel estimation. We then present an approximation for the average bit error probability by taking channel estimation errors into account. Simulations using SPW (Signal Processing WorkSystem, Cadence) are performed to compare with the analytical results.

2 System Model with Spatial and Temporal Channel Correlations

The system model considered here is that of a convolutionally coded DS-CDMA system employing a coherent rake receiver. It is assumed that every user is received with equal average signal power at the base station, i.e., power control is implicitly considered to have eliminated the near-far effect due to the pathloss and also large-scale fading. However, the short-scale (such as Rayleigh) fading is assumed to remain uncompensated.

The wideband frequency-selective channel is modeled as a random delay, discrete 'resolvable' path model [11]. The number of resolvable paths of the channel for the k-th user is assumed to be $L^{(k)}$. The received signal over each path is temporally correlated due to imperfect interleaving and channel correlation. In most analytical studies, the different paths are generally assumed to be mutually independent. However, when the resolvable delay between two consecutive paths becomes smaller (especially in the case of systems with relatively high chip rates as in WCDMA), the fading signals in two consecutive paths could be correlated. Such correlation may come from either the spatial correlation between two paths with small delay spread or the unresolvable paths due to pulse shaping filtering. Also, in the situation of antenna diversity, the correlation between different rake fingers may come from the spatial correlation between different antennas due to limited antenna spacing. In this paper, we do not distinguish the correlation between paths due to different reasons but simply characterize such correlation as spatial correlation. Thus, both the temporal correlation in each fading path and the spatial correlation between different fading paths could exist and affect the

coding performance.

2.1 Temporal Channel Correlation

For the k-th user, the envelope of each path in the wideband channel is assumed to be Rayleigh distributed. Thus, the sample value of each path at time iT (time index i) is a complex Gaussian random variable given as

$$h_l^{(k)}(i) = h_{xl}^{(k)}(i) + jh_{yl}^{(k)}(i), \quad 1 \le l \le L^{(k)}, \tag{1}$$

where T is the sample period, $h_{xl}^{(k)}(i)$ and $h_{yl}^{(k)}(i)$ represent respectively the I and Q components of the l-th path at time index i of the k-th user. The temporal autocorrelation function of $h_l^{(k)}(i)$ is given as [12]

$$\rho_{ll}^{(k)}(m) = \frac{1}{2}E[h_l^{(k)}(i)(h_l^{(k)}(i+m))^*] = (\sigma_{hl}^{(k)})^2 J_0(2\pi f_D m T), \quad 1 \le l \le L^{(k)}, \tag{2}$$

where f_D is the maximum Doppler frequency and $J_0(\cdot)$ is the zero-order Bessel function.

2.2 Spatial Channel Correlations

The spatial (cross) correlation coefficient between two Rayleigh faded envelopes $r_l^{(k)}(i) = |h_l^{(k)}(i)|$ and $r_n^{(k)}(i) = |h_n^{(k)}(i)|$ is expressed as (page 51 in [12])

$$\rho_r^{(k)} = \frac{(1+\lambda_{ln}^{(k)})E_i(\frac{2\sqrt{\lambda_{ln}^{(k)}}}{1+\lambda_{ln}^{(k)}}) - \frac{\pi}{2}}{2 - \frac{\pi}{2}} \tag{3}$$

where $\lambda_{ln}^{(k)}$ denotes the correlation coefficient between the complex amplitudes $h_l^{(k)}(i)$ and $h_n^{(k)}(i)$, and $E_i(\eta)$ denotes the complete elliptical integral of the second kind. The spatial and temporal correlation function between two complex amplitudes with time index difference m can be expressed as

$$\rho_{ln}^{(k)}(m) = \frac{1}{2}E[h_l^{(k)}(i)(h_n^{(k)}(i+m))^*] = \lambda_{ln}^{(k)}\sigma_{hl}^{(k)}\sigma_{hn}^{(k)}J_0(2\pi f_D m T), \quad 1 \le l \le L^{(k)}. \tag{4}$$

Readers are referred to [12] for further details and [13] for the algorithm for the generation of Rayleigh fading signals with spatial correlation.

3 Bit Error Probability Analysis

In this section, we analyze the bit error probability of a convolutional code with maximum-ratio combining (MRC) rake receiver in DS-CDMA systems. We first consider the case of perfect channel estimation and derive an upper bound for the average probability of bit error under both spatial and temporal channel correlations.

3.1 Upper bound for average bit error probability under perfect channel estimation

It is well known that the output of the maximum-ratio combining (MRC) rake receiver with channel estimation $\hat{h}_l^*(i)$ can be expressed as [6–8]

$$U(i) = Re\{\sum_{l=1}^{L}(\sqrt{E_s}h_l(i)b(i) + w_l(i))\hat{h}_l^*(i)\} \tag{5}$$

in the case of BPSK data modulation with $b(i) \in \{-1, +1\}$ being the modulated data symbol and E_s being the symbol energy. In the above equation and henceforth, we drop the super-index notation (k) and refer to the reference user only. Using the Gaussian assumption for the interference from $(K-1)$ users, the total interference $w_l(i) = w_{xl}(i)+jw_{yl}(i)$ is a complex white Gaussian variable with zero mean and variance $I_0/2$ [7, 8]

$$\sigma_w^2 = \frac{1}{2}E[w_l(i)w_l^*(i)] = \frac{I_0}{2} = (K-1)\frac{E_c}{2} + \frac{N_0}{2} \tag{6}$$

where $E_c = E_s/g = RE_b/g$ is the chip energy with g being the processing gain, E_b being the bit energy, and R being the code rate.

When the transmitted codeword is all-zero codeword C_0, a Viterbi decoder will select the erroneous codeword C_j if the received signal's Euclidean distance to C_j is less than that to C_0 [9, 10], i.e.,

$$\sum_{i=1}^{N}[U(i) - b_j(i)]^2 < \sum_{i=1}^{N}[U(i) - b_0(i)]^2 \tag{7}$$

where $U(i)$ is the soft input of the Viterbi decoder given in equation (5), $b_j(i)$ and $b_0(i)$ are the data symbols that correspond respectively to $C_j(i)$ and $C_0(i)$. Assuming that codewords

C_j and C_0 differ in d_j code-symbols and these positions are at $i_n, n = 1, 2, ...d_j$, the inequality in (7) can be shown to be equivalent to [8]

$$\sum_{n=1}^{d_j} Re\{\sum_{l=1}^{L}(\sqrt{E_s}h_l(i_n) + w_l(i_n))\hat{h_l}^*(i_n)\} < 0. \tag{8}$$

Under the assumption of perfect channel estimation, $\hat{h_l}(i_n)$ equals to $h_l(i_n)$. Following the derivation in [8], the average pairwise error probability can be expressed as

$$\overline{P}_{d_j}(C_j, C_0) = E\left[Q\left(\sqrt{2\frac{E_s}{I_0}\sum_{n=1}^{d_j}\sum_{l=1}^{L}|h_l(i_n)|^2}\right)\right] \tag{9}$$

where $E(\cdot)$ denotes the expectation over the set of random variables $\{h_l(i_n)\}_{l=1,...L;n=1,...d_j}$.

To obtain an upper bound for $\overline{P}_{d_j}(C_j, C_0)$ over a correlated channel, we follow a method similar to the one used by Gagnon and Haccoun in [9] for a temporally correlated Rician channel. However, both spatial and temporal correlations of the multipath signals are considered in our analysis. Using $Q(\sqrt{x}) \leq \frac{1}{2}\exp(-\frac{x}{2})$, an upper bound can be obtained as

$$\overline{P}_{d_j}(C_j, C_0) \leq \frac{1}{2}E\left[\exp\left(-\frac{E_s}{I_0}\sum_{n=1}^{d_j}\sum_{l=1}^{L}|h_l(i_n)|^2\right)\right]. \tag{10}$$

It can be rewritten as

$$\overline{P}_{d_j}(C_j, C_0) \leq \frac{1}{2}E\left[\exp\left(-\frac{E_s}{I_0}V_jV_j^\top\right)\right] \tag{11}$$

using the expression

$$V_j = [\ h_1 \quad h_2 \quad \ldots \quad h_L\ ] \tag{12}$$

with

$$h_l = [\ h_{xl} \quad h_{yl}\ ] = [\ h_{xl}(i_1) \quad \ldots \quad h_{xl}(i_{d_j}) \quad h_{yl}(i_1) \quad \ldots \quad h_{yl}(i_{d_j})\ ]. \tag{13}$$

Note that the symbol $\top$ represents the matrix transpose operator in equation (11). Since the components in row vector V_j are all zero-mean Gaussian random variables, it can be shown (using a technique in [14]) that

$$\frac{1}{2}E\left[\exp\left(-\frac{E_s}{I_0}V_jV_j^\top\right)\right] \quad = \quad \frac{1}{2|\frac{2E_s}{I_0}\mathbf{M}_j + \mathbf{I}_j|^{\frac{1}{2}}} \tag{14}$$

where $\mathbf{I}_j$ is the identity matrix of the same size as $\mathbf{M}_j$, and $\mathbf{M}_j$ is the autocovariance matrix of vector V_j defined as

$$\begin{aligned} \mathbf{M}_j &= E[(V_j - \overline{V_j})^\top (V_j - \overline{V_j})] = E[V_j^\top V_j] \\ &= \begin{pmatrix} \mathbf{M}_{11} & \mathbf{M}_{12} & \dots & \mathbf{M}_{1L} \\ \mathbf{M}_{21} & \mathbf{M}_{22} & \dots & \mathbf{M}_{2L} \\ \vdots & \vdots & \ddots & \vdots \\ \mathbf{M}_{L1} & \mathbf{M}_{L2} & \dots & \mathbf{M}_{LL} \end{pmatrix} \end{aligned} \tag{15}$$

with

$$\mathbf{M}_{ln} = E[h_l^\top h_n], \quad 1 \le l, n \le L. \tag{16}$$

The diagonal terms, $\mathbf{M}_{ll}, 1 \le l \le L$, are due to the temporal correlation in each path and can be calculated from $\rho_{ll}(m)$ in equation (2). The off-diagonal terms, $\mathbf{M}_{ln}, 1 \le l \ne n \le L$ are due to both the temporal correlation in each path and spatial correlations between different paths and can be calculated from $\rho_{ln}(m)$ in equation (4).

Thus the average pairwise error probability can be bounded as

$$\overline{P}_{d_j}(C_j, C_0) \le \frac{1}{2|\frac{2E_s}{I_0}\mathbf{M}_j + \mathbf{I}_j|^{\frac{1}{2}}}. \tag{17}$$

Using the well known union bound [11], the average bit error probability $\overline{P}_b$ can now be bounded as

$$\overline{P}_b \le \frac{1}{k}\sum_{j=1}^{\infty} \frac{B_j}{2|\frac{2E_s}{I_0}\mathbf{M}_j + \mathbf{I}_j|^{\frac{1}{2}}} \tag{18}$$

where B_j is the weight of information bits corresponding to codeword C_j, and the code rate is $R = k/n$. This upper bound for the average bit error probability is general enough to be applied to different spatial and temporal channel models, such as MIMO channel with spatial correlation [1, 3] and WSSUS (Wide Sense Stationary Uncorrelated Scattering) channel without spatial correlation [15].

3.2 Approximation of average bit error probability under channel estimation errors

We now consider the analytical results for the average probability of bit error when the channel estimates are not exact. Since the focus of this paper is not on any specific channel estimation technique, we use a general channel estimation error model in the analysis [16]. Specifically, the channel estimate, $\hat{h}_l(i)$, is modeled as

$$\hat{h}_l(i) = h_l(i) + e_l(i) \tag{19}$$

where $e_l(i) = e_{xl}(i) + je_{yl}(i)$ is a complex Gaussian random variable with mean $E[e_l(i)] = 0$ and variance $\sigma_{e_l}^2 = \frac{1}{2}E[e_l(i)e_l^*(i)]$. The error term $e_l(i)$ is assumed to be independent of $h_l(i)$. In the analysis of the average bit error probability that follows in this paper, we assume that $\sigma_{e_l}^2$ is known.

Starting from equation (8), the average pairwise error probability can be approximated as

$$\overline{P}_{d_j}(C_j, C_0) \approx E\left[Q\left(\sqrt{\frac{2\frac{E_s}{I_0}}{1 + 2\frac{E_s}{I_0}\bar{\sigma}_e^2 + 2L\bar{\sigma}_e^2}\sum_{n=1}^{d_j}\sum_{l=1}^{L}|h_l(i_n)|^2}\right)\right] \tag{20}$$

where $\bar{\sigma}_e^2$ is the average channel estimation error variance over multiple rake fingers. The details of the above derivation can be found in the Appendix. Similarly, the average bit error probability $\overline{P}_b$ under the channel estimation errors can be approximated as

$$\overline{P}_b \approx \frac{1}{k}\sum_{j=1}^{\infty}\frac{B_j}{2|\frac{2E_s/I_0}{1+2\frac{E_s}{I_0}\bar{\sigma}_e^2+2L\bar{\sigma}_e^2}\mathbf{M}_j + \mathbf{I}_j|^{\frac{1}{2}}}. \tag{21}$$

3.3 Calculation of the average bit error probability under block interleaving

In order to calculate the upper bound and the approximation of average bit error probability, the autocovariance matrix $\mathbf{M}_j$ needs to be calculated for different codewords C_j. In this section, we give an example on how to compute the autocovariance matrix $\mathbf{M}_j$ and also point out the effect of block interleaving.

For codeword C_j of a given convolutional code, the positions $i_n, n = 1, 2, ...d_j$, where C_j and C_0 have different code-symbols, can be obtained by an exhaustive binary-tree search [17]. Once these parameters are determined, the autocovariance matrix $\mathbf{M}_j$ can be calculated. Now we illustrate this for the example of a convolutional code (1/2, 3) (rate 1/2 and constraint length 3). The generator polynomial of this code is (5 7) in octal format [17]. This code has a free distance of 5. Considering a pair codewords $C_1 = (1\ 1\ 0\ 1\ 1\ 1)$ and $C_0 = (0\ 0\ 0\ 0\ 0\ 0)$, the two codewords differ in $d_j = 5$ positions $i_n = \{1, 2, 4, 5, 6\}, n = 1, 2, ...5$. Since the I and Q components of the same path are assumed to be mutually independent, the diagonal terms of the autocovariance matrix $\mathbf{M}_1$ (corresponding to codeword C_1) can be calculated as

$$\mathbf{M}_{ll} = E[h_l^\top h_l] = \begin{pmatrix} \Phi_{ll} & \mathbf{0} \\ \mathbf{0} & \Phi_{ll} \end{pmatrix}, \quad l = 1, 2...L, \tag{22}$$

with

$$\begin{aligned} \Phi_{ll} &= E[h_{xl}^\top h_{xl}] = E[h_{yl}^\top h_{yl}] \\ &= \begin{pmatrix} \rho_{ll}(0) & \rho_{ll}(1) & \rho_{ll}(3) & \rho_{ll}(4) & \rho_{ll}(5) \\ \rho_{ll}(1) & \rho_{ll}(0) & \rho_{ll}(2) & \rho_{ll}(3) & \rho_{ll}(4) \\ \rho_{ll}(3) & \rho_{ll}(2) & \rho_{ll}(0) & \rho_{ll}(1) & \rho_{ll}(2) \\ \rho_{ll}(4) & \rho_{ll}(3) & \rho_{ll}(1) & \rho_{ll}(0) & \rho_{ll}(1) \\ \rho_{ll}(5) & \rho_{ll}(4) & \rho_{ll}(2) & \rho_{ll}(1) & \rho_{ll}(0) \end{pmatrix} \end{aligned} \tag{23}$$

where the autocorrelation function $\rho_{ll}(m)$ is defined in equation (2). The off-diagonal terms $\mathbf{M}_{ln}, 1 \leq l \neq n \leq L$, can be calculated similarly using $\rho_{ln}(m)$ in equation (4). Therefore, the autocovariance matrix $\mathbf{M}_1$ can be obtained. From $\mathbf{M}_1$ the upper bound or approximation of the average pairwise error probability $\overline{P}_{d_j}(C_1, C_0)$ can be calculated. Similarly, the average pairwise error probability $\overline{P}_{d_j}(C_j, C_0)$ for other pairs of codewords can be calculated. Thus the upper bound or approximation of the average bit error probability $\overline{P}_b$ can be evaluated using equation (18) and (21), respectively.

Interleaving is commonly used to reduce or break the correlation of errors caused by fading channels. However, perfect interleaving is not always feasible due to delay constraints

and hardware memory limits especially for high data rates. With imperfect interleaving, the received signals of adjacent symbols are temporally correlated. As pointed out in [9,10,18], a slowly fading system with interleaving is equivalent to a faster fading system without interleaving. Consider a commonly used block interleaver with interleaving depth D and interleaving length N, where N is assumed to be large enough to avoid the "wraparound" effect [7], which is the situation when in a code word two code symbols separated by N-1 code symbols at the receiver are consecutive during transmission. After interleaving/deinterleaving, two adjacent code symbols at the receiver are separated by another $D-1$ code symbols during transmission over the channel. For a fading channel with normalized Doppler frequency of $f_D T_s$, after interleaving/deinterleaving, the equivalent normalized Doppler frequency becomes $f_D(DT_s)$ [9,18]. Thus for interleaved systems, the normalized Doppler frequency $f_D T_s$ in $\rho_{ll}(m)$ and $\rho_{ln}(m)$ should be replaced by $f_D(DT_s)$ in the calculation of the autocovariance matrix $\mathbf{M}_j$.

4 Numerical Results

In this section, the average bit error probability results are presented for a convolutionally coded DS-CDMA system with a coherent rake receiver. In these examples, we consider two standard convolutional codes, a (1/2, 7) code (rate 1/2 and constraint length 7) with generator polynomial (133 171) in octal form and a (1/3, 9) code with generator polynomial (557 663 711) in octal form [11, 17].

Figure 1 shows the upper bound for the average bit error probability ($\overline{P}_b$) for (1/2, 7) code under perfect channel estimation and different interleaving depth. Here the interleaving length N is chosen to be 32 and the interleaving depth D is 51, 101 and 404 for interleaving delay of 10ms, 20ms and 80ms respectively. For this example, the channel model is composed of $L = 4$ mutually uncorrelated paths with equal average power. The Doppler frequency is 51.67Hz. The frame size is 10ms. The channel symbol rate is 161.1 ksps (kilo-symbols per second). All the above parameters are chosen to match the parameters used in Figure 6 of the reference [8] for comparison. This code has a free distance $d_f = 10$ and only even Hamming

weight codewords. For this example, the upper bound for the average bit error probability $\overline{P}_b$ in equation (18) is calculated using only codewords having the Hamming distance 10, 12 and 14 from the all-zero codeword C_0. Further the numbers of codewords with Hamming distance 10, 12, and 14 are 11, 38 and 193 respectively [17]. The total number of these codewords is 242, or equivalently the number of terms used in the upper bound calculation in equation (18) is 242. Our simulation results using SPW are also shown to compare with our analytical results. It is observed that our upper bounds are relatively tight for different interleaving depths. Also, our simulation results match well to the simulation results of Figure 6 in reference [8]. It is noticed that the upper bound for $\overline{P}_b$ is not asymptotically tight when E_b/N_0 increases. This is because the exponential function is used to upper bound the $Q(\cdot)$ function and as such the exponential function is not an asymptotically tight bound of the $Q(\cdot)$ function. In spite of this, the upper bound is still reasonably tight.

Figure 2 shows the upper bound and simulation results for (1/3, 9) code under perfect channel estimation and two different Doppler frequencies. This code is used in practical DS-CDMA systems such as IS-95 and WCDMA. This code has a free distance $d_f = 18$ and only even Hamming weight codewords. The upper bound for the average bit error probability $\overline{P}_b$ is calculated using the codewords having three lowest Hamming distances, i.e., 18, 20, and 22, from the all-zero codeword C_0. The total number of these codewords is 48. Again, the results show that the upper bound analysis works well for different Doppler frequencies.

The upper bound and simulation results of $\overline{P}_b$ in Figure 3 show the degradation of $\overline{P}_b$ due to spatial correlation between different rake fingers. For instance, when the cross-correlation coefficient λ equals 0.7 ($\rho_r = 0.49$) as shown in this example, the degradation is about 1.0dB compared to the case with mutually uncorrelated (independent) rake fingers.

Figure 4 shows the analytical approximation and simulation results of $\overline{P}_b$ under channel estimation error and different Doppler frequencies. The spatial correlation is assumed to be zero here, i.e., $\lambda = 0$. Note that the analytical approximations have a good match to the simulation results.

Figure 5 shows the analytical approximation and simulation results of $\overline{P}_b$ with temporal and spatial correlation as well as channel estimation errors. Again, the analytical approx-

imations of $\overline{P}_b$ have a good match to the simulation results. Our results indicate that the analytical approximation underestimates those from simulations when the channel estimation error variance σ_e^2 is larger and the spatial and temporal channel correlation is higher. This is due to the approximation in equation (30) in Appendix.

The effect of correlated errors on $\overline{P}_b$ due to imperfect interleaving (temporal correlation only) can be seen from Figure 1 and 2. For the (1/2,7) code shown in Figure 1, the degradation from 80ms interleaving to 10ms interleaving can be as large as 2dB at $\overline{P}_b = 10^{-3}$ and 4dB at $\overline{P}_b = 10^{-6}$. Similar degradations due to smaller Doppler frequencies can be seen for the (1/3, 9) code in Figure 2. For voice applications at $\overline{P}_b = 10^{-3}$, this degradation may be inevitable due to the delay constraint of voice applications. For non-real time data applications, longer interleaving is preferred for significant performance improvement.

The impact of channel estimation errors on $\overline{P}_b$ can be seen more easily from the analytical results in Figure 6. In this example, the channel with mutually independent 4 equal power Rayleigh paths is considered. The variance of each Rayleigh signal, σ_h^2, equals 0.125 due to the normalized power of total signals. In our analysis and simulations, we have used a constant channel estimation error variance for different E_s/I_0 values. In practice, the channel estimation error variance will generally decrease with an increase in E_s/I_0. Also the channel estimation error will be affected by the fading rate of the channel. However the focus of this paper is not on any specific channel estimation method. Figure 6 indicates that once the variance of the channel estimation error is obtained, it can be incorporated with our analytical method to evaluate the performance of convolutionally coded DS-CDMA systems.

5 Conclusion

Space-time processing is a promising technique to increase the link capacity of wireless communication systems. Various techniques such as maximum-ratio rake finger combining and antenna diversity, have been used in DS-CDMA systems to improve the performance and capacity. Considering both temporal and spatial channel correlations encountered in space-time processing and the channel estimation errors, we have presented the performance

analysis of convolutionally coded DS-CDMA systems. We derived an upper bound for the average bit error probability ($\overline{P}_b$) in the case of perfect channel estimation and an analytical approximation for $\overline{P}_b$ in the case of erroneous channel estimates. The analytical approach is general enough to be applicable to various space and time diversity situations, such as wideband multipath channels and antenna arrays. The analytical results are obtained as a succinct function of the weight distribution of the codeword, temporal and spatial channel correlation values and are able to account for channel estimation errors when applicable.

Appendix. The approximation of the pairwise error probability with channel estimation errors

From the inequality in equation (8), the average pairwise error probability can be derived as follows under the situation of channel estimation errors. Firstly, the LHS of equation (8) can be written as

$$\sum_{n=1}^{d_j} Re\{\sum_{l=1}^{L}(\sqrt{E_s}h_l(i_n) + w_l(i_n))\hat{h_l}^*(i_n)\} = s_t + w_t \tag{24}$$

where the signal component s_t is given as

$$s_t = \sqrt{E_s}\sum_{n=1}^{d_j}\sum_{l=1}^{L}|h_l(i_n)|^2 \tag{25}$$

and the noise component w_t is given as

$$\begin{aligned} w_t \;=\; & \sum_{n=1}^{d_j}\sum_{l=1}^{L}[w_{xl}(i_n)h_{xl}(i_n) + w_{yl}(i_n)h_{yl}(i_n) + \sqrt{E_s}h_{xl}(i_n)e_{xl}(i_n) + \sqrt{E_s}h_{yl}(i_n)e_{yl}(i_n) \\ & + w_{xl}(i_n)e_{xl}(i_n) + w_{yl}(i_n)e_{yl}(i_n)]. \end{aligned} \tag{26}$$

The conditional power in the signal component s_t, denoted as $P_{s_t}|\{h_l(i_n)\}$, is given as

$$P_{s_t}|\{h_l(i_n)\} = E_s(\sum_{n=1}^{d_j}\sum_{l=1}^{L}|h_l(i_n)|^2)^2. \tag{27}$$

We approximate the noise w_t conditioned on $\{h_l(i_n)\}_{l=1,\ldots L;n=1,\ldots d_j}$ as a Gaussian random variable with zero mean, denoted as $E[w_t|\{h_l(i_n)\}] = 0$ and variance

$$\sigma^2_{w_t}|\{h_l(i_n)\} = \sigma^2_w \sum_{n=1}^{d_j}\sum_{l=1}^{L}|h_l(i_n)|^2 + E_s\sum_{n=1}^{d_j}\sum_{l=1}^{L}\sigma^2_{el}|h_l(i_n)|^2 + \sum_{n=1}^{d_j}\sum_{l=1}^{L}2\sigma^2_w\sigma^2_{el}. \quad (28)$$

Let us denote the average channel estimation error variance as $\bar{\sigma}^2_e = \frac{1}{L}\sum_{l=1}^{L}\sigma^2_{el}$. The second term in the expression for $\sigma^2_{w_t}|\{h_l(i_n)\}$ (equation (28)) is now approximated as

$$E_s\sum_{n=1}^{d_j}\sum_{l=1}^{L}\sigma^2_{el}|h_l(i_n)|^2 \approx E_s\bar{\sigma}^2_e\sum_{n=1}^{d_j}\sum_{l=1}^{L}|h_l(i_n)|^2. \quad (29)$$

The last term in the expression for $\sigma^2_{w_t}|\{h_l(i_n)\}$ (equation (28)) can be expressed as

$$\begin{aligned}\sum_{n=1}^{d_j}\sum_{l=1}^{L}2\sigma^2_w\sigma^2_{el} &= 2L\sigma^2_w\bar{\sigma}^2_e\sum_{n=1}^{d_j}\sum_{l=1}^{L}|h_l(i_n)|^2 + 2L\sigma^2_w\bar{\sigma}^2_e\sum_{n=1}^{d_j}(1-\sum_{l=1}^{L}|h_l(i_n)|^2)\\ &\approx 2L\sigma^2_w\bar{\sigma}^2_e\sum_{n=1}^{d_j}\sum_{l=1}^{L}|h_l(i_n)|^2. \quad (30)\end{aligned}$$

Thus $\sigma^2_{w_t}|\{h_l(i_n)\}$ can be approximated by

$$\sigma^2_{w_t}|\{h_l(i_n)\} \approx (\sigma^2_w + E_s\bar{\sigma}^2_e + 2L\sigma^2_w\bar{\sigma}^2_e)\sum_{n=1}^{d_j}\sum_{l=1}^{L}|h_l(i_n)|^2 \quad (31)$$

The conditional pairwise error probability can be calculated as

$$\begin{aligned}P_{d_j}(C_j, C_0|\{h_l(i_n)\}) &\approx Q\left(\sqrt{\frac{P_{s_t}|\{h_l(i_n)\}}{\sigma^2_{w_t}|\{h_l(i_n)\}}}\right)\\ &\approx Q\left(\sqrt{\frac{2\frac{E_s}{I_0}}{1+2\frac{E_s}{I_0}\bar{\sigma}^2_e+2L\bar{\sigma}^2_e}\sum_{n=1}^{d_j}\sum_{l=1}^{L}|h_l(i_n)|^2}\right). \quad (32)\end{aligned}$$

The unconditional average pairwise error probability can be expressed as

$$\overline{P}_{d_j}(C_j, C_0) \approx E\left[Q\left(\sqrt{\frac{2\frac{E_s}{I_0}}{1+2\frac{E_s}{I_0}\bar{\sigma}^2_e+2L\bar{\sigma}^2_e}\sum_{n=1}^{d_j}\sum_{l=1}^{L}|h_l(i_n)|^2}\right)\right] \quad (33)$$

where the expectation $E(\cdot)$ is over the channel $\{h_l(i_n)\}_{l=1,\ldots L;n=1,\ldots d_j}$.

References

[1] G. J. Foschini and G. J. Gans, "On the limits of wireless communications in a fading environment when using multiple antennas," *Wireless Personal Communications*, vol. 6, pp. 311–335, Mar. 1998.

[2] V. Tarokh, N. Seshadri, and A. R. Calderbank, "Space-time codes for high data rate wireless communication: Performance criterion and code construction," *IEEE Trans. on Information Theory*, vol. 44, pp. 744–765, Mar. 1998.

[3] S. L. Ariyavisitakul, "Turbo space-time processing to improve wireless channel capacity," *IEEE Trans. on Communications*, vol. 48, pp. 1347–1359, Aug. 2000.

[4] W. C.-Y. Lee, "Effects on correlation between two mobile radio base-station antennas," *IEEE Trans. on Communications*, vol. 21, no. 11, pp. 1214–1224, 1973.

[5] S. Affes and P. Mermelstein, "Performance of a CDMA beamforming array-receiver in spatially-correlated Rayleigh-fading multipath," in *Proceedings of VTC'99*, pp. 249–253, 1999.

[6] T. Eng and L. B. Milstein, "Coherent DS-CDMA performance in Nakagami multipath fading," *IEEE Trans. on Communications*, vol. 43, pp. 1134–1143, Feb./Mar./Apr. 1995.

[7] F. Simpson and J. M. Holtzman, "Direct sequence CDMA power control, interleaving, and coding," *IEEE J. Selected Areas in Communications*, vol. 11, pp. 1085–1095, Sept. 1993.

[8] R. Cideciyan, E. Eleftheriou, and M. Rupf, "Concatenated Reed-Solomon/convolutional coding for data transmission in CDMA-based cellular systems," *IEEE Trans. on Communications*, vol. 45, pp. 1291–1303, Oct. 1997.

[9] F. Gagnon and D. Haccoun, "Bounds on the error performance of coding for nonindependent Rician-fading channels," *IEEE Trans. on Communications*, vol. 40, pp. 351–360, Feb. 1992.

[10] R. Nobelen and D. Taylor, "Analysis of the pairwise error probability of noninterleaved codes on the Rayleigh-fading channel," *IEEE Trans. on Communications*, vol. 44, pp. 456–463, April 1996.

[11] J. Proakis, *Digital Communications*. McGraw Hill, 3rd ed., 1995.

[12] W. C. Jakes, Jr., *Microwave Mobile Communications*. New York: John Wiley and Sons, 1974.

[13] R. B. Ertel and J. H. Reed, "Generation of two equal power correlated Rayleigh fading envelops," *IEEE Communications Letters*, vol. 2, pp. 276–278, Oct. 1998.

[14] G. L. Turin, "The characteristic function of Hermitian quadratic forms in complex normal variables," *Biometrika*, vol. 47, pp. 190–201, June 1960.

[15] P. Hoeher, "A statistical discrete-time model for the WSSUS multipath channel," *IEEE Trans. on Vehicular Technology*, vol. VT-41, pp. 461–468, Nov. 1992.

[16] P. K. Frenger, N. Arne, and B. Svensson, "Decision directed coherent detection in multicarrier systems on Rayleigh fading channels," *IEEE Trans. on Vehicular Technology*, vol. 48, pp. 490–498, Mar. 1999.

[17] J. Conan, "The weight spectra of some short low-rate convolutional codes," *IEEE Trans. on Communications*, vol. COM-32, pp. 1050–1053, Sept. 1984.

[18] J. Lai and N. B. Mandayam, "Performance of Reed-Solomon codes for hybrid-ARQ over Rayleigh fading channels under imperfect interleaving," *IEEE Trans. on Communications*, vol. 48, pp. 1650–1659, Oct. 2000.

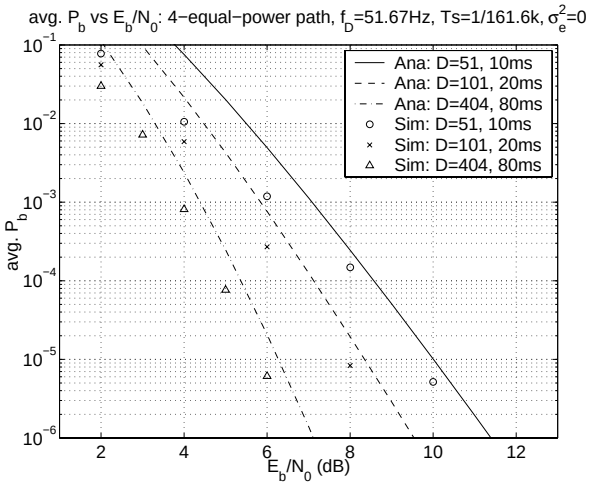

Figure 1: The upper bound and simulation results of $\overline{P}_b$ for different interleaving under perfect channel estimation ($\sigma_e^2 = 0$). (1/2, 7) code, mutually independent 4-equal-power channel ($L = 4$), $f_D = 51.67$Hz, channel rate $1/T_s = 161.1$ ksps, frame size = 10ms, block interleaver $N = 32, D = 51, 101, 404$.

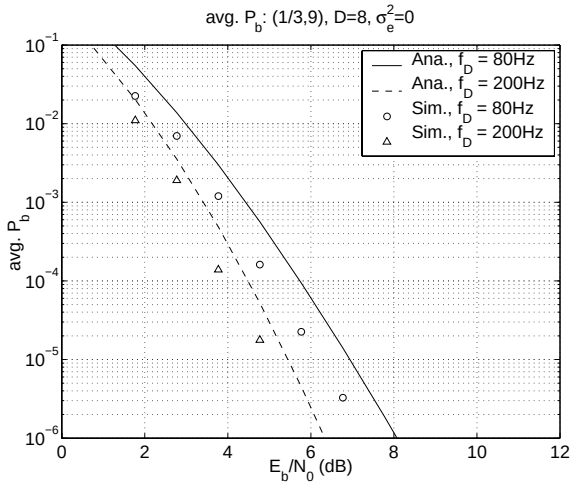

Figure 2: The upper bound and simulation results of $\overline{P}_b$ for different Doppler frequencies under perfect channel estimation ($\sigma_e^2 = 0$). (1/3, 9) code, mutually independent 4-equal-power channel ($L = 4$), f_D =80, 200Hz, channel rate $1/T_s = 28.8$ ksps, block size = 20ms, block interleaver $N = 72, D = 8$.

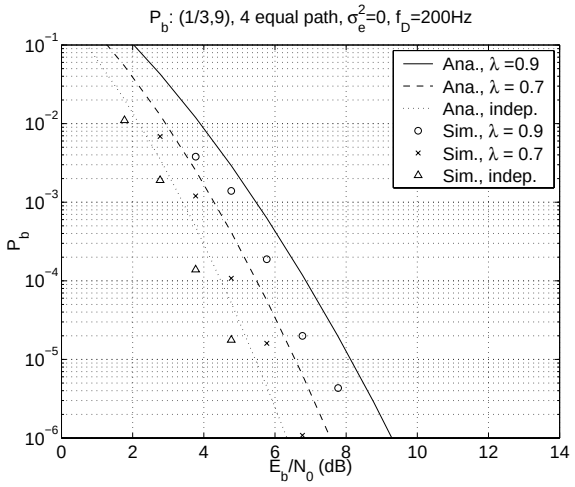

Figure 3: The upper bound and simulation results of $\overline{P}_b$ with spatial correlation between different fading paths under perfect channel estimation. (1/3, 9) code, spatially correlated 4-equal-power channel ($L = 4$), $f_D = 200$Hz, channel rate $1/T_s = 28.8$ ksps, block size = 20ms, block interleaver $N = 72, D = 8$, $\sigma_e^2 = 0$.

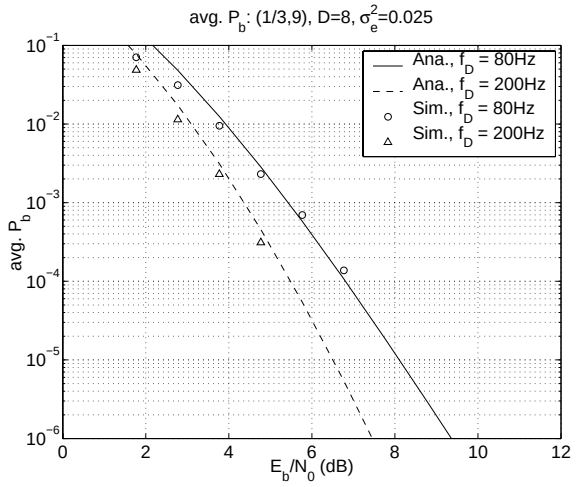

Figure 4: The analytical approximation and simulation results of $\overline{P}_b$ under channel estimation error and different Doppler frequencies. (1/3, 9) code, mutually independent 4-equal-power channel ($L = 4$), $f_D = 80$, 200Hz, channel rate $1/T_s = 28.8$ ksps, block size = 20ms, block interleaver $N = 72, D = 8$, $\sigma_e^2 = 0.025$.

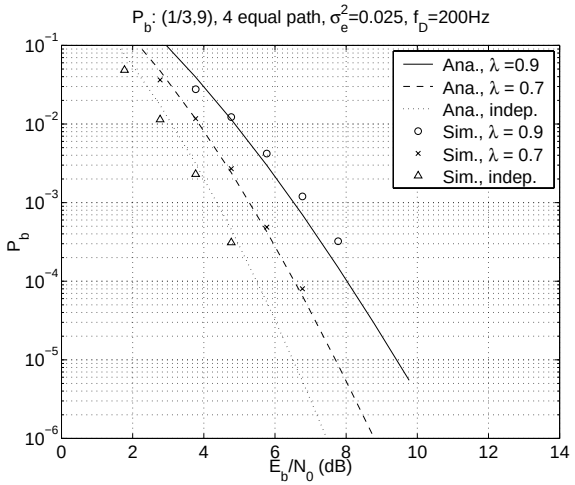

Figure 5: The analytical approximation and simulation results of $\overline{P}_b$ with spatial correlation and channel estimation errors. (1/3, 9) code, spatially correlated 4-equal-power channel ($L = 4$), $f_D = 200$Hz, channel rate $1/T_s = 28.8$ ksps, block size = 20ms, block interleaver $N = 72, D = 8$, $\sigma_e^2 = 0.025$.

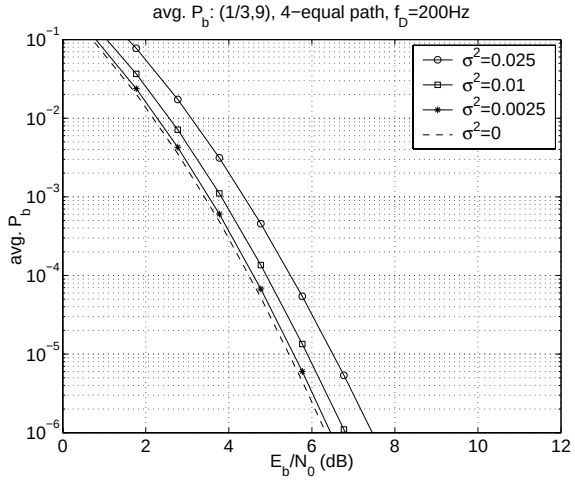

Figure 6: The analytical results of degradation of $\overline{P}_b$ due to different channel estimation error variances. (1/3,9) code, mutually independent 4-equal-power channel ($L = 4$), $f_D =$ 200Hz, channel rate $1/T_s = 28.8$ ksps, block size = 20ms, block interleaver $N = 72, D = 8$.